

Production of W bosons in p-Pb collisions measured with ALICE at the LHC

Edith Zinhle Buthelezi¹

for the ALICE Collaboration

*iThemba Laboratory for Accelerator Based Sciences
Old Faure Road, Faure, 7131, Western Cape, South Africa
E-mail: edith.zinhle.buthelezi@cern.ch*

W bosons, which are produced in hard scattering processes of partons in collisions of hadrons, do not interact strongly with the medium produced in high-energy heavy-ion collisions. Therefore, in p-Pb collisions the measurement of W-boson yields represents a standard candle to check the validity of binary scaling and can provide important constraints on the parton distribution functions, which can be modified in nuclei with respect to protons or neutrons.

At the LHC, ALICE (A Large Ion Collider Experiment) is dedicated to the study of ultra-relativistic heavy-ion collisions, in which a hot and dense, strongly-interacting medium is formed. At forward rapidity ALICE is equipped with a muon spectrometer that allows measurements of dimuon decays of quarkonia, muons from heavy-flavour hadron decays and also W bosons via their single-muon decay. In ALICE W-boson cross sections were measured in p-Pb collisions at $\sqrt{s_{NN}} = 5.02$ TeV via the contribution of their muonic decays to the inclusive p_T -differential muon yield measured at forward ($2.03 < y_{cms}^\mu < 3.53$) and backward ($-4.46 < y_{cms}^\mu < -2.96$) rapidity. Recent results obtained from these measurements are presented and compared to perturbative Quantum Chromodynamics calculations at next-to-leading order.

*XXIII International Workshop on Deep-Inelastic Scattering and Related Subjects
Dallas, Texas (27 April - May 1 2015)*

¹Speaker

© Copyright owned by the author(s) under the terms of the Creative Commons Attribution-NonCommercial-NoDerivatives 4.0 International License (CC BY-NC-ND 4.0).

1. Introduction

Electroweak W bosons were discovered at the CERN Super Proton Synchrotron (SPS) in the early [1]. They are massive particles ($80.385 \pm 0.015 \text{ GeV}/c^2$) produced in initial hard parton scattering processes with a formation time of approximately $0.003 \text{ fm}/c$ and have a lifetime of about $0.09 \text{ fm}/c$ [2]. Their properties have been studied extensively at hadron colliders [3]. In proton-proton collisions their cross sections are known with a precision limited by the parton distribution function (PDF) uncertainties. The measurements of W bosons via the leptonic decay channels (branching ratios of $10.57 \pm 0.15\%$) are not affected by the presence of strongly-interacting matter. The unprecedented energies available at the Large Hadron Collider (LHC) make it possible to measure W bosons in pp, Pb-Pb and p-Pb collisions and will allow to probe parton distribution functions and their nuclear modification at Bjorken- x ranges $x \sim (10^{-4} - 10^{-1})$ at large scales $Q^2 = M_W^2/2$ [4]. In p-Pb collisions the measurements of their yields allow the investigation of cold nuclear matter effects and constrain nuclear parton distribution functions (nPDF) [5][6]. Also, they serve as an important baseline for the understanding and the interpretation of Pb-Pb data.

In this report, preliminary results are presented obtained with ALICE from the study of W-boson production in the single muon decay channel, $W^\pm \rightarrow \mu^\pm \nu$, at forward ($2.03 < y_{cms}^\mu < 3.53$) and backward ($-4.46 < y_{cms}^\mu < -2.96$) rapidity for muons with transverse momentum $p_T^\mu > 10 \text{ GeV}/c$ in p-Pb collisions at $\sqrt{s_{NN}} = 5.02 \text{ TeV}$. The measurements are compared to predictions from pQCD calculations at next-to-leading-order (NLO) [5] and are complementary to results recently published by the CMS Collaboration [7].

2. Experimental setup and data sample

As the detailed description of the ALICE detector is given in [8][9] here parts of the detector used in the present measurements are briefly described. ALICE comprises of central barrel detectors embedded in a solenoid magnet ($B = 0.5 \text{ T}$) covering the pseudo-rapidity of $|\eta| < 0.9$ where hadrons, electrons and photons are measured, and a forward muon spectrometer. Information on global event characterization is provided by the VZERO detectors, which are two plastic scintillators, V0A and V0C, situated on either side of the interaction point at $2.8 < \eta < 5.1$ and $-3.7 < \eta < -1.7$, the two layers of the Silicon Pixel Detector (SPD) located in the central barrel and the Zero Degree Calorimeters, ZNA and ZNC, located at a distance of 112 m on either side of the interaction point along the beam pipe. The VZERO detector is also used for triggering as well as for offline rejection of beam-gas events while the SPD is also used to determine the interaction vertex. The muon spectrometer, located at $-4.0 < \eta < -2.5$, is composed of a passive front absorber of 10 interaction lengths ($10 \lambda_{int}$) designed to filter hadrons, photons, electrons and muons from light hadron decays before the spectrometer, a dipole magnet providing a field integral of 3 Tm , five tracking stations each composed of two planes of Cathode Pad Chambers, a muon filter which absorbs most of the punch-through hadrons and lastly, the two trigger stations equipped with two planes of Resistive Plate Chambers located downstream of the tracking system.

The analysis is based on data collected in 2013 in p-Pb collisions at $\sqrt{s_{NN}} = 5.02 \text{ TeV}$. Due to the LHC design, the colliding beams have different energies per nucleon: $E_p = 4 \text{ TeV}$, $E_{pb} =$

42 1.58 A_{Pb} TeV ($A_{\text{Pb}} = 208$ is the mass number of the Pb nucleus). Consequently, the centre-of-
 43 mass of the nucleon-nucleon collision is shifted by $\Delta y = 0.465$ with respect to the laboratory
 44 frame in the direction of the proton beam. Data were taken in two configurations by inverting
 45 the orbits of the two beams. In this way, both forward ($2.03 < y_{\text{cms}}^{\mu} < 3.53$) and backward
 46 ($-4.46 < y_{\text{cms}}^{\mu} < -2.96$) nucleon-nucleon centre-of-mass rapidities are covered, with the
 47 positive rapidity defined by the direction of the proton beam. The integrated luminosities for p-
 48 Pb and Pb-p collisions are 4.9 nb^{-1} and 5.8 nb^{-1} , respectively. The data sample consists of
 49 minimum bias trigger events (MB - coincidence of a signal in both the event counters and the
 50 VZERO detectors) and tracks in the muon trigger system with $p_{\text{T}} \geq 4 \text{ GeV}/c$. An offline
 51 selection is applied and events without a reconstructed primary vertex from the SPD are
 52 rejected. Furthermore, tracks are required to be reconstructed within the acceptance of the muon
 53 spectrometer: $-4.0 < \eta_{\text{lab}} < -2.5$, $170^{\circ} < \theta_{\text{abs}} < 178^{\circ}$, where θ_{abs} is the polar angle at the end
 54 of the absorber. To eliminate tracks from punch-through hadrons each track candidate of interest
 55 in the tracking system is required to match the corresponding track reconstructed in the trigger
 56 system. Finally, a $p\text{DCA}$ cut (correlation of the momentum, p , and the distance of closest
 57 approach, DCA) is applied within 6σ , where σ is the standard deviation of the distribution in
 58 order to remove fake, beam-gas tracks and particles produced in the absorber.

59 3. Data analysis

60 In the analysis the W-boson signal, i.e. the number of muons from the decays of W bosons,
 61 $N_{\mu\leftarrow\text{W}}$, is extracted by taking into account the contributions of $\text{W}^+ \rightarrow \mu^+ \nu_{\mu}$ and $\text{W}^- \rightarrow \mu^- \bar{\nu}_{\mu}$ to the
 62 inclusive single-muon p_{T} distributions. The decay kinematic provides two final state particles
 63 with $p_{\text{T}} \sim \frac{M_{\text{W}}}{2} \sim 40 \text{ GeV}/c$. Since the neutrino cannot be detected, the signature is a high- p_{T}
 64 muon with a large missing transverse energy and it is characterized by a p_{T} distribution which
 65 dominates inclusive muon yield at $p_{\text{T}} > 30 \text{ GeV}/c$, with a Jacobean peak at $p_{\text{T}} \sim 40 \text{ GeV}/c$. The
 66 main sources of background contributing to the inclusive p_{T} spectra are semi-muonic decays of
 67 heavy-flavour (charm and beauty hadrons) which dominate at $10 < p_{\text{T}} < 35 \text{ GeV}/c$ [4] as well as
 68 dimuons from Z^0/γ^* decays which populate the region of $p_{\text{T}} > 50 \text{ GeV}/c$. The yield of muons
 69 from W-boson decays is extracted by fits based on suitable parameterizations of the different
 70 components. The components of W and Z-boson decays are described by using [10] based on
 71 next-to-leading-order Monte Carlo (MC) event generator templates [10] with CT10 [14] PDF
 72 and PYTHIA [11] to take into account the [12] nuclear modification of the PDF. The isospin is
 73 accounted for in the template by generating pp and pn collisions and combining the results using

$$\frac{dN_{p\text{Pb}}}{dp_{\text{T}}} = \frac{Z}{A} \frac{1}{N_{pp}} \frac{dN_{pp}}{dp_{\text{T}}} + \frac{A-Z}{A} \frac{1}{N_{pn}} \frac{dN_{pn}}{dp_{\text{T}}} \quad (1)$$

A = 208 and Z = 82 are mass and atomic number of the Pb nucleus, respectively. The different
 contributions are taken into account and summed together in the final fit function defined by

74

$$f(p_{\text{T}}) = N_{\text{bkg}} f_{\text{bkg}}(p_{\text{T}}) + N_{\mu\leftarrow\text{W}} f_{\mu\leftarrow\text{W}}(p_{\text{T}}) + N_{\mu\leftarrow\text{Z}/\gamma^*} f_{\mu\leftarrow\text{Z}/\gamma^*}(p_{\text{T}}) \quad (2)$$

75

76 where $f_{\text{bkg}}(p_{\text{T}})$ represent templates for muons from heavy-flavour decays based on a pQCD
 77 calculation at fixed-order-next-to-leading-log (FONNL) [13], $f_{\mu\leftarrow\text{W}}(p_{\text{T}})$ and $f_{\mu\leftarrow\text{Z}/\gamma^*}(p_{\text{T}})$ are
 78 templates for W and Z/ γ^* components based on POWHEG [10]. The free parameters are N_{bkg}

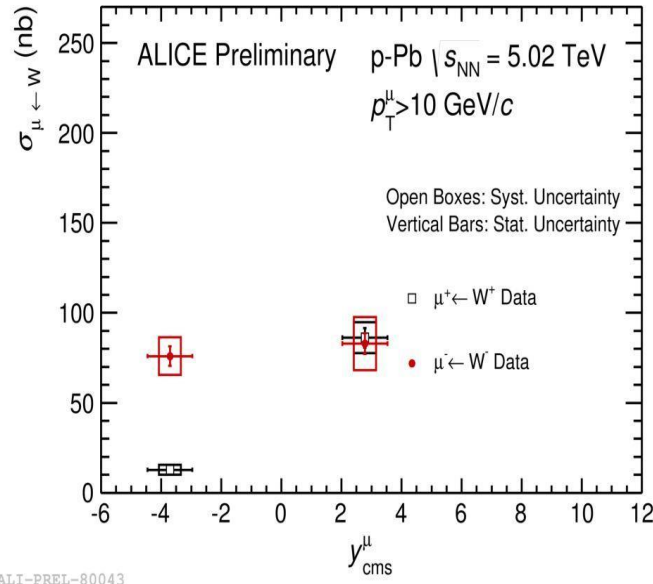
79 and $N_{\mu \leftarrow W}$ which are the number of muons from heavy-flavour decays and W bosons,
 80 respectively, while $N_{\mu \leftarrow Z/\gamma^*}$, i.e. the number of muons from Z/γ^* decays, is not a free parameter
 81 in the fit; it is fixed to the number of muons from W decays, $N_{\mu \leftarrow W}$. Furthermore, the signal is
 82 corrected for acceptance and efficiency using POWHEG [10] simulations. Finally, $N_{\mu \leftarrow W}$ is
 83 normalized to the number of minimum bias (MB) events. The systematic uncertainties
 84 associated with the signal extraction account for $\sim 6 - 24\%$, tracking and trigger efficiency
 85 $\sim 2.5\%$, detector alignment accounts for $\sim 1\%$, normalization to MB events $\sim 7.2\%$ and up to
 86 8.6% to account for pile-up effects.

87 4. Results

88 Preliminary results for the production cross sections, $\sigma_{\mu \leftarrow W}$, of muons from W-boson decays
 89 obtained in this analysis are presented in two rapidity intervals, forward ($2.03 < y_{cms}^\mu < 3.53$)
 90 and backward ($-4.46 < y_{cms}^\mu < -2.96$) in Figure 1. The isospin effects are clearly visible, i.e. at
 91 backward rapidity (Pb ion beam direction) an enhancement is seen for W^- where $\sigma_{\mu \leftarrow W^-}$ is
 92 larger than $\sigma_{\mu \leftarrow W^+}$ whereas at forward rapidity $\sigma_{\mu \leftarrow W^-}$ is approximately equal to $\sigma_{\mu \leftarrow W^+}$. This
 93 could potentially arise from chirality, i.e. the production of W^+ is suppressed because the proton
 94 beam is coming from the spectrometer side (negative rapidity) and W^+ is boosted towards the
 95 direction of the proton. In Figure 2 the same results are compared with POWHEG [10]
 96 predictions which do not include nuclear shadowing effects (nPDF). Predictions by POWHEG
 97 [10] slightly over-estimate $\sigma_{\mu \leftarrow W^+}$. For $\sigma_{\mu \leftarrow W^-}$ the agreement is good. In Figure 3 and Figure 4
 98 we compare the measured cross sections with pQCD theoretical predictions [5] at next-to-
 99 leading order (NLO) assuming both unmodified (CT10) [14] and modified (CT10+EPS09[12])
 100 nPDFs. Taking into account the EPS09 prescription of nuclear shadowing of the PDFs further
 101 improves the agreement between data and theory, especially at the forward rapidity. These
 102 results are also consistent with observations made by the CMS collaboration [7].

103 5. Summary

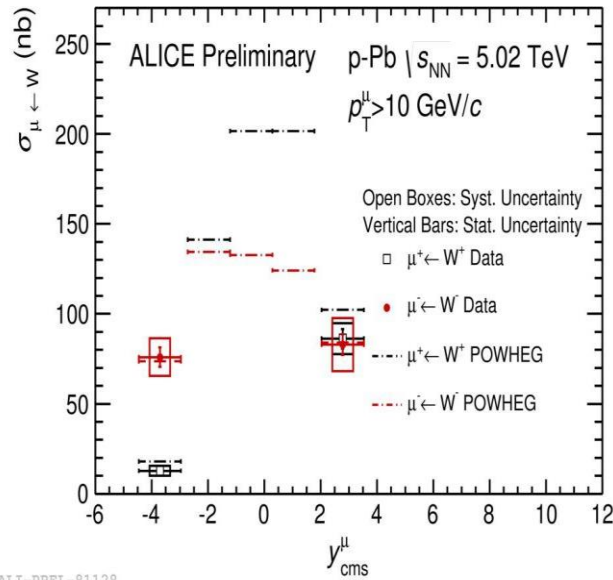
104 We have measured W-boson production via the single-muon decay channel at forward and
 105 backward rapidity in p-Pb collisions at $\sqrt{s_{NN}} = 5.02$ TeV. The comparison of experimental
 106 results with theoretical calculations shows a good agreement within uncertainties. Further
 107 improvements are seen when taking into account the EPS09 prescription of nuclear shadowing
 108 of the PDFs. These results are consistent with what has been observed by the CMS
 109 Collaboration [7] and they complement the rapidity range covered at the LHC. The
 110 measurements will be useful to further constrain pQCD calculations as suggested in [5].
 111



112

ALI-PREL-80043

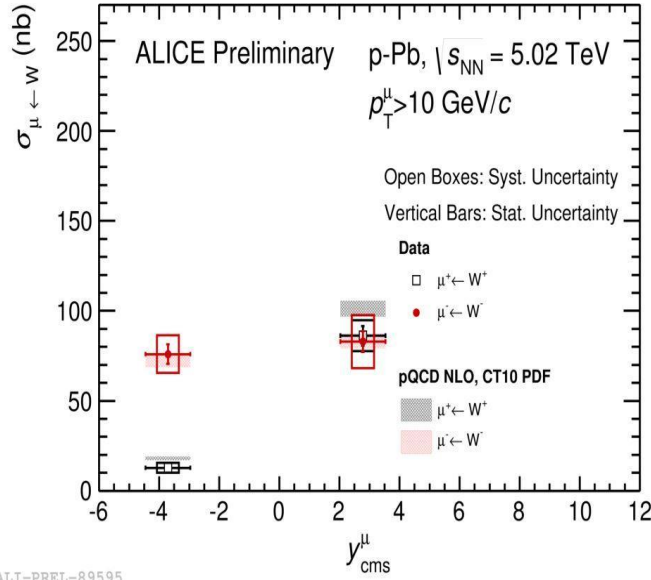
Figure 1 : Cross sections of W- boson production at forward and backward rapidity in p-Pb collisions at $\sqrt{s_{NN}} = 5.02$ TeV.



113

ALI-PREL-81128

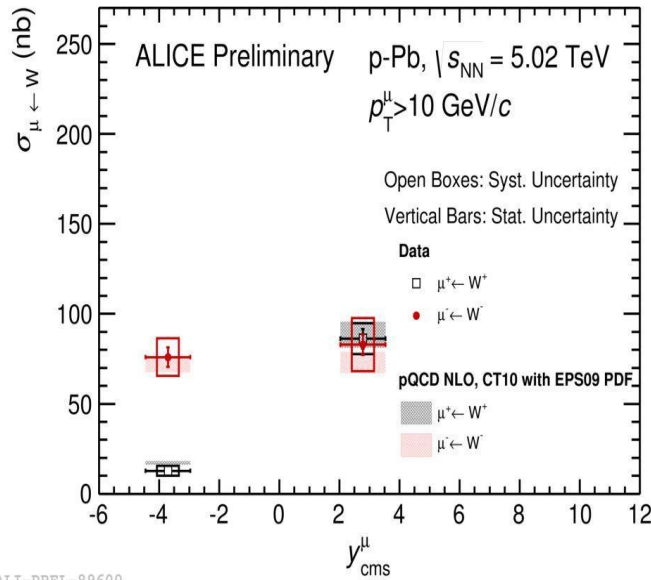
Figure 2 : Cross sections of W-boson production at forward and backward rapidity in p-Pb collisions at $\sqrt{s_{NN}} = 5.02$ TeV compared with predictions by [10]



114

ALI-PREL-89595

Figure 3 : Cross sections of W-boson production at forward and backward rapidity in p-Pb collisions at $\sqrt{s_{\text{NN}}} = 5.02$ TeV compared with theoretical predictions based on pQCD NLO with CT10 [14].



115

ALI-PREL-89600

Figure 4 : Cross sections of W-boson production at forward and backward rapidity in p-Pb collisions at $\sqrt{s_{\text{NN}}} = 5.02$ TeV compared with theoretical predictions based on pQCD NLO with CT10 [14] and EPS09 PDF from [12].

116

117 Acknowledgements

118 The author would like to thank the Department of Science and Technology of South
119 Africa, the National Research Foundation and iThemba LABS for financial support.

120 **References**

- 121 [1] G. Arnison et al., *Phys. Lett. B* 122 (1983) 103.
- 122 [2] J. Beringer, et al., *Phys. Rev. D* 86 (2012) 010001.
- 123 [3] W-M Yao, et al., *J. Phys. G* 33 (2006) 1.
- 124 [4] Z Conesa del Valle, *Eur. Phys. J. C* 6 (2009) 729-733.
- 125 [5] Hannu Paukkunen and Carlos A. Salgado, *JHEP* 1103 (2011) 071.
- 126 [6] Peng Ru, Ben-Wei Zhang, Luan Cheng, Enke Wang, Wei-Ning Zhang, *J. Phys. G: Nucl. Part. Phys.*
127 42 (2015) 085104.
- 128 [7] The CMS Collaboration, *arXiv: 1503.05825 [nucl-ex]*.
- 129 [8] The ALICE Collaboration, *J. Instrum.* 3, (2008) S08002.
- 130 [9] The ALICE Collaboration, *Int. J. Phys. Z* 29 (2014) 1430044.
- 131 [10] S. Alioli, P. Nason, C. Oleari, E. Re, *JHEP* 0807 (2008) 060.
- 132 [11] Torbjörn Sjöstrand, Stephen Mrenna and Peter Skands, *JHEP* 05 (2006) 026.
- 133 [12] K.J. Eskola, H. Paukkunen and C.A. Salgado, *JHEP* 0904 (2009) 065.
- 134 [13] M. Cacciari, S. Frixione, N. Houdeau, M.L Mangano, P Nason, et al., *JHEP* 1210 (2012) 137.
- 135 [14] Hung-Lai Lai, Guzzi Marco et al., *Phys. Rev. D* 82 (2012) 074024.